

AD-A038 625

GENERAL APPLIED SCIENCE LABS INC WESTBURY N Y  
THE EFFECTS OF VISCOUS INTERACTION ON THE TRANSONIC JET-FLAP.(U)  
MAR 77 P BARONTI, S ELZWEIG, G MILLER

F/G 1/3

F44620-76-C-0017

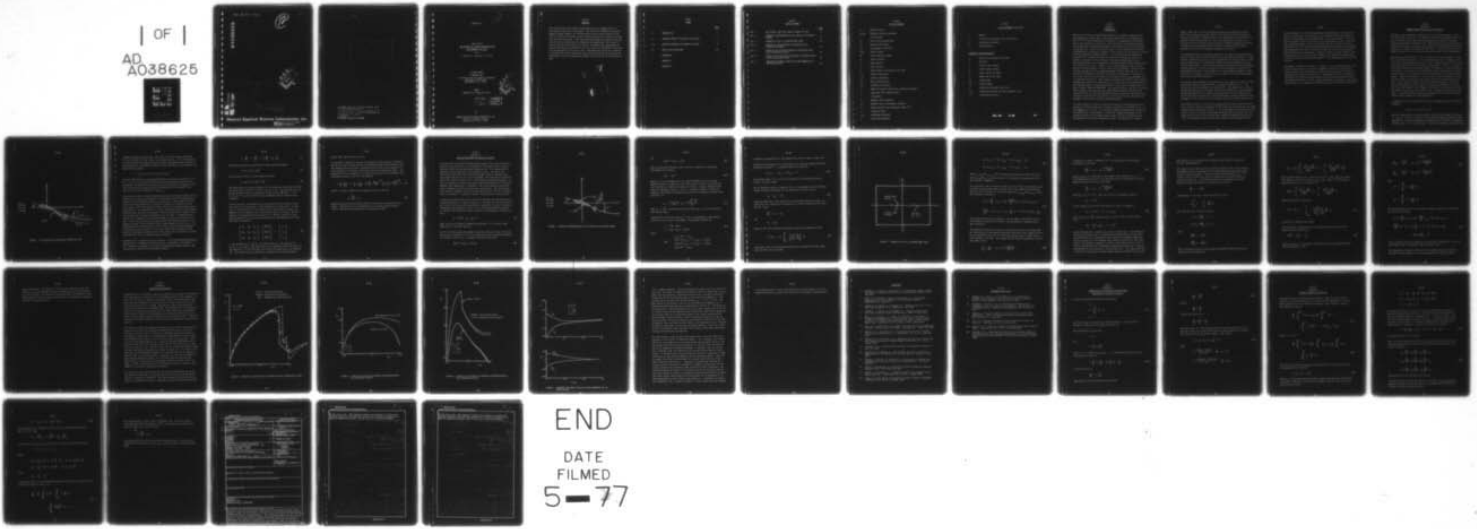
UNCLASSIFIED

GASL-TR-237

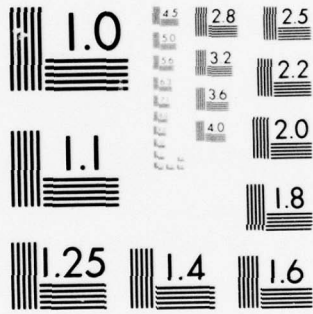
AFOSR-TR-77-0446

NL

| OF |  
AD  
A038625



END  
DATE  
FILMED  
5-77



MICROCOPY RESOLUTION TEST CHART  
NATIONAL BUREAU OF STANDARDS-1963-A

*J*

*(12)*

AD A 038625



*See from 1472*

DDC  
APR 25 1977  
ASDC

AD No. \_\_\_\_\_  
DDC FILE COPY

DISTRIBUTION STATEMENT A  
Approved for public release;  
Distribution Unlimited

**General Applied Science Laboratories inc.**

Approved for public release;  
distribution unlimited.



AIR FORCE OFFICE OF SCIENTIFIC RESEARCH (AFSC)  
NOTICE OF TRANSMITTAL TO DDC  
This technical report has been reviewed and is  
approved for public release IAW AFR 190-12 (7b).  
Distribution is unlimited.  
A. D. ELOSE  
Technical Information Officer

12

MARCH 1977

GASL TR 237  
THE EFFECTS OF VISCOUS INTERACTION ON  
THE TRANSONIC JET-FLAP

BY

P. Baronti, S. Elzweig & G. Miller

A FINAL REPORT  
PREPARED FOR  
AIR FORCE OFFICE OF SCIENTIFIC RESEARCH  
BOLLING AIR FORCE BASE  
WASHINGTON, D. C. 20332

UNDER  
CONTRACT NO. F44620-76-C-0017

DDC  
APR 25 1977  
ALULC

**DISTRIBUTION STATEMENT A**  
Approved for public release;  
Distribution Unlimited

By

GENERAL APPLIED SCIENCE LABORATORIES, INC.  
Merrick and Stewart Avenues  
Westbury, New York 11590

TR 237  
ABSTRACT

The inviscid and viscous effects associated with a jet-flapped airfoil in the transonic regime are investigated. The particular formulation developed employs integral methods for the description of the viscous portions of the flow (utilizing the turbulent kinetic energy equation) and a relaxation method for the inviscid portions. The viscous-inviscid coupling procedures along the wing and the jet acknowledge the importance and magnitude of the viscous effects on pressure distribution and directly incorporate the displacement effect on the wing and the effects of the jet mixing into the boundary conditions for the computation of the entire flow. Some numerical results are presented to validate the solution techniques that have been selected and to assess the importance of mass and momentum entrainment into the jet on jet flap effectiveness.

ADDITIONAL INFO	White Screen	<input checked="" type="checkbox"/>
NTIS	Full Screen	<input type="checkbox"/>
DDI	Full Screen	<input type="checkbox"/>
SEARCHED		
INDEXED		
SERIALIZED		
FILED		
APR 1980		
NTIS		
DISTRIBUTION STATEMENTS		
1. UNANNOUNCED		
2. ANNOUNCED		
3. BOTH ANNOUNCED AND UNANNOUNCED		
4. NOT FOR DISTRIBUTION		
5. EXCLUDED FROM DISTRIBUTION		
6. OTHER		
7. UNCLASSIFIED		
8. CLASSIFIED		
9. UNCLASSIFIED		
10. CLASSIFIED		
11. UNCLASSIFIED		
12. CLASSIFIED		
13. UNCLASSIFIED		
14. CLASSIFIED		
15. UNCLASSIFIED		
16. CLASSIFIED		
17. UNCLASSIFIED		
18. CLASSIFIED		
19. UNCLASSIFIED		
20. CLASSIFIED		
21. UNCLASSIFIED		
22. CLASSIFIED		
23. UNCLASSIFIED		
24. CLASSIFIED		
25. UNCLASSIFIED		
26. CLASSIFIED		
27. UNCLASSIFIED		
28. CLASSIFIED		
29. UNCLASSIFIED		
30. CLASSIFIED		
31. UNCLASSIFIED		
32. CLASSIFIED		
33. UNCLASSIFIED		
34. CLASSIFIED		
35. UNCLASSIFIED		
36. CLASSIFIED		
37. UNCLASSIFIED		
38. CLASSIFIED		
39. UNCLASSIFIED		
40. CLASSIFIED		
41. UNCLASSIFIED		
42. CLASSIFIED		
43. UNCLASSIFIED		
44. CLASSIFIED		
45. UNCLASSIFIED		
46. CLASSIFIED		
47. UNCLASSIFIED		
48. CLASSIFIED		
49. UNCLASSIFIED		
50. CLASSIFIED		
51. UNCLASSIFIED		
52. CLASSIFIED		
53. UNCLASSIFIED		
54. CLASSIFIED		
55. UNCLASSIFIED		
56. CLASSIFIED		
57. UNCLASSIFIED		
58. CLASSIFIED		
59. UNCLASSIFIED		
60. CLASSIFIED		
61. UNCLASSIFIED		
62. CLASSIFIED		
63. UNCLASSIFIED		
64. CLASSIFIED		
65. UNCLASSIFIED		
66. CLASSIFIED		
67. UNCLASSIFIED		
68. CLASSIFIED		
69. UNCLASSIFIED		
70. CLASSIFIED		
71. UNCLASSIFIED		
72. CLASSIFIED		
73. UNCLASSIFIED		
74. CLASSIFIED		
75. UNCLASSIFIED		
76. CLASSIFIED		
77. UNCLASSIFIED		
78. CLASSIFIED		
79. UNCLASSIFIED		
80. CLASSIFIED		
81. UNCLASSIFIED		
82. CLASSIFIED		
83. UNCLASSIFIED		
84. CLASSIFIED		
85. UNCLASSIFIED		
86. CLASSIFIED		
87. UNCLASSIFIED		
88. CLASSIFIED		
89. UNCLASSIFIED		
90. CLASSIFIED		
91. UNCLASSIFIED		
92. CLASSIFIED		
93. UNCLASSIFIED		
94. CLASSIFIED		
95. UNCLASSIFIED		
96. CLASSIFIED		
97. UNCLASSIFIED		
98. CLASSIFIED		
99. UNCLASSIFIED		
100. CLASSIFIED		

TR 237

INDEX

	<u>Page</u>
I. INTRODUCTION	1
II. INTEGRAL METHOD FOR VISCOUS JET SOLUTION	4
III. COUPLING PROCEDURE FOR COMPLETE SOLUTION	9
IV. RESULTS AND CONCLUSIONS	20
REFERENCES	
APPENDIX A	
APPENDIX B	

TR 237  
LIST OF FIGURES

		<u>Page</u>
FIG. 1.	THE VISCOUS FLOW FIELD ALONG A CURVED JET FLAP	5
FIG. 2.	SCHEMATIC REPRESENTATION OF THE INVISCID JET-FLAPPED AIRFOIL	10
FIG. 3.	SCHEMATIC OF THE $\xi, \eta$ COMPUTATIONAL PLANE	13
FIG. 4.	EFFECTS OF VISCOUS-INVISCID INTERACTION ON 6% CIRCULAR-ARC AIRFOIL	21
FIG. 5.	EFFECT OF JET MIXING ON PRESSURE DISTRIBUTION OVER A 6% CIRCULAR-ARC AIRFOIL	22
FIG. 6.	EFFECT OF JET VISCOSITY ON PRESSURE DISTRIBUTION OVER A 12% CIRCULAR-ARC AIRFOIL	23
FIG. 7.	PRESSURES AND NORMAL VELOCITIES ALONG BOUNDARIES OF JET MIXING REGION	24

LIST OF SYMBOLS

$a$	speed of sound
$a_i, G, L$	Bradshaw turbulent parameters
$c$	airfoil chord
$c_f$	skin friction coefficient
$c_p$	pressure coefficient
$c_j$	jet momentum coefficient
$f(x)$	airfoil shape
$M_\infty$	free stream Mach number
$p$	static pressure
$P$	wake function
$q$	total velocity
$R$	local radius of curvature of jet flap
$s, n$	natural coordinates
$u, v$	velocity components
$U_\infty$	free stream velocity
$x, y$	Cartesian coordinates
$\alpha$	angle of attack of wing, also stretching parameter
$\beta$	functional form, Equation (19)
$\Gamma$	circulation
$\delta$	boundary layer thickness
$\delta^*$	boundary layer displacement thickness
$\theta$	angle related to jet curvature, Figure (2)
$\nu$	relaxation step
$\xi, \eta$	stretched coordinates
$\pi$	Coles wake parameter

TR 237

LIST OF SYMBOLS (Continued)

$\rho$  density  
 $\tau$  initial jet flap angle, also shear stress  
 $\phi$  perturbation potential  
 $\psi$  stream function

SUBSCRIPTS AND SUPERSCRIPTS

e condition at boundary layer edge  
j jet flap  
l airfoil lower surface  
u airfoil upper surface  
B lower side of jet sheet  
T upper side of jet sheet  
LE leading edge  
TE trailing edge  
o condition along base line of jet  
1,2 conditions at upper and lower boundary of jet  
— transformed variables

TR 237  
SECTION I  
INTRODUCTION

The use of jet flaps to enhance maneuverability in transonic flight has been under scrutiny in recent years. Wind tunnel experiments on jet-flapped airfoils<sup>1,2,3,4,5</sup> have indicated that significant lift augmentation and improvement of the drag polar at large lift can be obtained in the transonic regime; at the same time, retardation of boundary layer separation and of buffet onset can be achieved. A body of theoretical work is also available which provides a mathematical and numerical framework for the solution of the transonic inviscid flow field around jet-flapped airfoils. Ives and Melnick<sup>6</sup> have numerically solved the full transonic potential equation while allowing the jet flap to maintain a constant, finite, thickness. Malmuth and Murphy have given a linearized solution for two-dimensional<sup>7</sup> and three-dimensional<sup>8</sup> jet-flapped wings with infinitely thin jets. However, none of these analytical models has explored the viscous effects of the jet on airfoil performance, since jet mixing has been excluded and the jet momentum assumed constant along the jet. As originally indicated by Stratford,<sup>9</sup> the effect of entrainment is to cause the jet to act like a sink with respect to the inviscid field, with consequent loss of recoverable jet thrust. More recently, Yoshihara and Zonars<sup>10</sup> have reviewed, although qualitatively, the effects of jet viscosity on jet flap performance in the transonic regime. They have pointed out, on the basis of experimental evidence, several important phenomena: the ejector action of the jet in increasing trailing edge suction (and thus decreasing thrust recovery), the effective reduction of the jet exit angle because of jet mixing, and the importance of jet and wake viscous-inviscid interaction in providing a realistic picture of the transonic flow field for large jet deflection angles.

For these reasons, an effort to assess the effects of viscous-inviscid interaction on jet effectiveness was initiated by the authors in Reference (11). An inviscid analysis, as well as an attendant computer program similar to that of Ives and Melnick, was developed. In addition, integral techniques for the separate analyses of the viscous regions along the airfoil and the jet were developed and the coupling procedures outlined. The choice of an integral

method, rather than a finite difference technique, was prompted by previous work<sup>12</sup> which showed that boundary layers over supercritical wings and wakes can be well treated by integral methods, once implemented by a solution of the turbulent kinetic energy equation. Also, the separation of the flow into inviscid and viscous regions greatly reduces the numerical/computational effort as compared to time-dependent solutions of the "turbulent" Navier-Stokes equations, which may be foreseeably attempted in the future.

In the present report, the integral solution of the viscous flow along the jet and the viscous-inviscid coupling along the jet have been reconsidered. Further numerical experimentation has in fact revealed that the integral solution of the viscous flow along the jet developed in Reference (11) was unstable when the jet was highly curved. This has necessitated the reformulation of the momentum integral equations in terms of velocity profiles expressed by polynomials of second degree (instead of third degree, as it was originally proposed in Reference (11)). In addition, a more consistent viscous-inviscid coupling procedure along the jet has been elaborated.

The present report completes the formulation of the problem of viscous-inviscid interaction along jet-flapped airfoils, initiated in Reference (11). The salient features of the method are reviewed here. They consist of an inviscid relaxation procedure that resembles that of Ives and Melnick, integral methods for the description of the viscous (turbulent) portions of the flow along the airfoil and along the curved jet, and an appropriate coupling procedure for the treatment of the viscous-inviscid interaction along the wing and along the jet.

The integral solution of the jet flap presented here suffers from some limitations, since it requires a modelling of the viscous jet flap which may not always be consistent with physical reality. In fact, the present representation of the velocity field at the wing trailing edge or equivalently at the jet exit, considers only the jet velocity profile and disregards the detailed velocity profiles of the boundary layers on both sides of the wing which merge with the

jet flow (however, in the actual computations performed here, the initial jet profile is modified so as to satisfy, on the average, the mass and momentum flux of the jet-boundary layer combination). This representation is realistic when the boundary layer on the wing is thin and attached, or when it has very small separated regions at the wing trailing edge, but it becomes invalid in the case of jets with large initial deflection angles which may induce boundary layer separation and large recirculation regions at the wing trailing edge.<sup>10</sup> Notwithstanding these limitations it appears, however, that the integral representation may be usefully and simply invoked for a quantitative determination of viscous effects on jet-flap performance in many configurations of practical interest.

The report is organized as follows. In Section II the integral analysis of the viscous region along a curved jet is presented. Section III outlines the inviscid analysis and the coupling procedure of the viscous and inviscid solutions along the wing and along the jet. Some numerical results, indicating the effects of jet-mixing and entrainment on the pressure distribution over a two-dimensional airfoil, as well as some conclusions with respect to the quantitative effect of jet momentum and deflection angle, are presented in Section IV.

INTEGRAL METHOD FOR VISCOUS JET SOLUTION

The authors have developed in Reference (11) an integral solution of the viscous flow along a curved jet. An integral solution of the boundary layer flow over an airfoil, under subcritical and supercritical conditions, had been previously developed in Reference (12). Both solutions utilize an integral solution of the turbulent kinetic energy equation<sup>13</sup> and simple coordinate transformations to account for compressibility effects. The formulation of the integral solution of the viscous region along a curved jet is now reconsidered.

With reference to Figure (1), a jet is issued from the trailing edge of an airfoil with a deflection angle  $\tau$ . The flow around the wing is assumed to be inviscid (thus the boundary layer over the wing is neglected) and only the mixing of the jet with the inviscid flow field is considered. A line  $s$ , not necessarily the centerline of the mixing region, is selected as a "base" streamline of the flow. Its position, to be determined by the viscous-inviscid coupling discussed below, can be proved<sup>14</sup> to be accurate to order  $\delta$  of boundary layer theory. Along this streamline  $v = 0$ , but, still within the accuracy of boundary layer theory, the velocity profile  $u(n)$  may have a slope different from zero. Thus, a shear different from zero is allowed along the  $s$ -streamline. The mixing boundaries of the curved jet, defined by the boundary lines  $n = \delta_1$  and  $n = \delta_2$ , are asymmetric with respect to the "base" streamline and the inviscid velocities  $u_1$  and  $u_2$  along  $\delta_1$  and  $\delta_2$  are, in general, different from each other. The problem solution requires a representation of velocity and shear profiles which accounts for these asymmetries.

In Reference (11), the velocity profiles were represented by the third degree polynomial

$$u = u_0 + a_1 n + a_2 n^2 + a_3 n^3$$

with the coefficients  $a_1$  and  $a_2$  defined by satisfying the boundary conditions  $u = u_1$  at  $n = \delta_1$  and  $u = u_2$  at  $n = \delta_2$  (note that the edge derivatives are left unspecified). The flow development was then defined in terms of the dependent variable  $u_0(s)$ ,  $\delta_1(s)$ ,  $\delta_2(s)$  and  $a_3(s)$ . These were obtained by integrating the

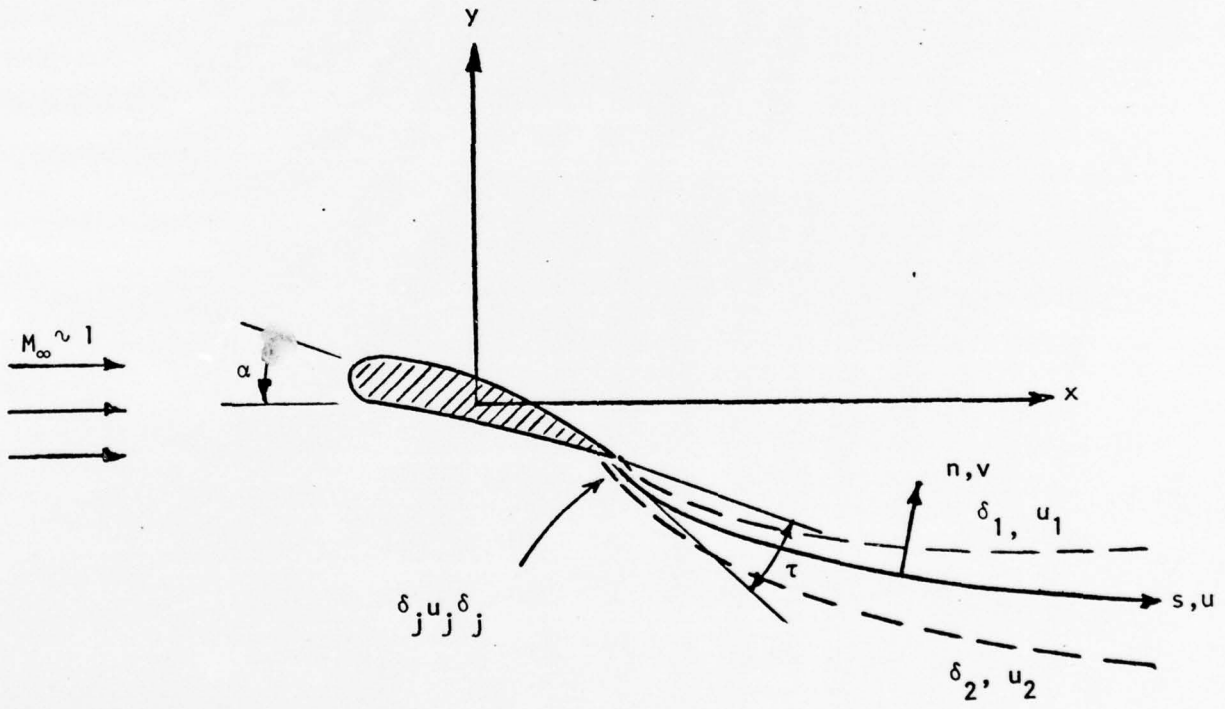


FIGURE 1. THE VISCOUS FLOW FIELD ALONG A CURVED JET FLAP

streamwise momentum equation four times, that is from the "base" streamline  $n = 0$  to  $\delta_1/2$  and to  $\delta_1$  and from  $n = 0$  to  $\delta_2/2$  and to  $\delta_2$ . In a similar fashion, in order to obtain the shear distribution across the boundary layer (needed in the integration of the momentum equation), shear profiles were prescribed by the fourth order polynomial

$$\tau = b_0 + b_1 n + b_2 n^2 + b_3 n^3 + b_4 n^4$$

with the coefficients  $b_1$ ,  $b_2$  and  $b_0$  obtained by satisfying the conditions  $\tau = 0$  at  $n = \delta_1$  and  $n = \delta_2$  and by satisfying the  $s$ -momentum equation along the base streamline. The coefficients  $b_3$  and  $b_4$  were then obtained by integrating twice the turbulent kinetic energy equation of Bradshaw, Ferris and Atwell<sup>15</sup> between  $n = 0$  and  $\delta_1$  and between  $n = 0$  and  $\delta_2$ .

The resulting system of integral momentum equations was analyzed extensively for asymmetric jet flows but was found to be unstable for cases of large deflection angles and large differences between  $u_1(s)$  and  $u_2(s)$ . The instabilities were traced to the representation of the velocity profiles by polynomials of the third degree, which could produce negative velocities and uncontrolled velocity amplifications. A representation of velocity and shear profiles by lower degree polynomials has then been investigated. Resort has been made to parabolic velocity profiles and third degree polynomials for the shear. An approach which utilizes the integration of the momentum equation in the three steps from 0 to  $\delta_1/2$ , from 0 to  $\delta_2/2$  and from  $\delta_1$  to  $\delta_2$  was then established and coupled to an integral solution of the turbulent kinetic energy equation from  $\delta_1$  to  $\delta_2$ . This system was found to be stable even for the case of severe asymmetries between the velocities  $u_1(s)$  and  $u_2(s)$ . It was also found to be as accurate as the previous system based on polynomials of third degree for the velocity, in those cases where the latter system gave stable solutions.

The details of the formulation are as follows. A restricted Dorodnitsyn-Howarth compressibility transformation (where only the  $n$  coordinate is stretched) is first invoked, see Appendix A, to yield the transformed momentum equation (barred quantities identify the transformed variables)

$$\bar{u} \frac{\partial \bar{u}}{\partial s} + \bar{v} \frac{\partial \bar{u}}{\partial n} = - \frac{1}{\rho} \frac{\partial \bar{p}}{\partial s} + \frac{1}{\rho} \frac{\partial \bar{\tau}}{\partial n} \quad (1)$$

The velocity profiles are described by a second degree polynomial

$$\bar{u} = \bar{u}_0 + a_1 \bar{n} + a_2 \bar{n}^2 \quad (2)$$

and the shear profile by a third degree polynomial

$$\bar{\tau} = b_0 + b_1 \bar{n} + b_2 \bar{n}^2 + b_3 \bar{n}^3 \quad (3)$$

The coefficients  $a_1$  and  $a_2$  in Equation (2) are defined by satisfying the boundary conditions  $\bar{u} = \bar{u}_1$  at  $\bar{n} = \bar{\delta}_1$  and  $\bar{u} = \bar{u}_2$  at  $\bar{n} = \bar{\delta}_2$ . The coefficients  $b_1$ ,  $b_2$  and  $b_0$  of Equation (3) are obtained by satisfying the conditions  $\bar{\tau} = 0$  at  $\bar{n} = \bar{\delta}_1$  and  $\bar{n} = \bar{\delta}_2$  and by satisfying the s-momentum equation along the base streamline.

A Crocco integral, see Appendix A, for the definition of the density variation across the viscous layer is then assumed to be locally valid. In addition, a linear variation of the pressure across the jet can be proved, see Appendix B, to be adequate even in the case of highly curved jets. The integration of the momentum equation, Equation (1), between 0 and  $\bar{\delta}_1/2$ , 0 and  $\bar{\delta}_2/2$  and between  $\delta_1$  and  $\delta_2$  can then be carried out, see Appendix B, to yield the system of equations

$$\begin{vmatrix} A_{11} & A_{12} & A_{13} \\ A_{21} & A_{22} & A_{23} \\ A_{31} & A_{32} & A_{33} \end{vmatrix} \begin{vmatrix} d\bar{u}_0/ds \\ d\bar{\delta}_1/ds \\ d\bar{\delta}_2/ds \end{vmatrix} = \begin{vmatrix} C_1 \\ C_2 \\ C_3 \end{vmatrix} \quad (4)$$

in the variables  $\bar{u}_0$ ,  $\bar{\delta}_1$  and  $\bar{\delta}_2$ . The coefficients  $A_{i,j}$  are functions of  $\bar{u}_0$ ,  $\bar{\delta}_1$ ,  $\bar{\delta}_2$ ,  $\bar{u}_1$  and  $\bar{u}_2$ . The coefficients  $C_i$  are functions also of the values of the shear at  $n = 0$ ,  $\bar{\delta}_1/2$  and  $\bar{\delta}_2/2$ , and thus of the coefficient  $b_3$  of Equation (3). The coefficient  $b_3$  is obtained by integrating the turbulent kinetic

energy, TKE, equation across the jet.

It was shown in Reference (12) that the compressible TKE equation of Bradshaw and Ferris<sup>16</sup> can be transformed by the Dorodnitsyn-Howarth transformation into the incompressible form given in Reference (15) and that such an equation, derived originally for boundary layer flows, can be also applied to wakes. The applicability of this equation to straight and curved jet is now assumed. Thus, integration between  $\bar{\delta}_1$  and  $\bar{\delta}_2$  of the equation

$$\bar{u} \frac{\partial}{\partial \bar{s}} \left( \frac{\bar{\tau}}{2a_1 \bar{\rho}} \right) + \bar{v} \frac{\partial}{\partial \bar{n}} \left( \frac{\bar{\tau}}{2a_1 \bar{\rho}} \right) - \frac{\bar{\tau}}{\bar{\rho}} \frac{\partial \bar{u}}{\partial \bar{n}} + \left( \frac{\bar{\tau}_{\max}}{\bar{\rho}} \right)^{1/2} \frac{\partial}{\partial \bar{n}} \left( G \frac{\bar{\tau}}{\bar{\rho}} \right) + \frac{(\bar{\tau}/\bar{\delta})^{3/2}}{\bar{L}} = 0 \quad (5)$$

yields, as shown in Appendix B, an equation for  $b_3$  of the form

$$B_1 \frac{db_3}{ds} = G_1 \quad (6)$$

Equations (4) and (6) provide the closure of the system of equations and unknowns. Application of the transformation in an inverse manner provides, finally, the desired flow quantities in the physical plane.

COUPLING PROCEDURE FOR COMPLETE SOLUTION

A viscous-inviscid coupling procedure which accounts for strong interaction along the wing and the jet is now developed. The boundary layer solution along the wing is the one developed in Reference (12). The viscous solution along the jet was presented in the preceding section. The details of the initial conditions at the wing trailing edge, where the boundary layer flow merges with the jet flow, are disregarded. The occurrence of separation and of recirculation regions at the trailing edge are excluded; however, initial jet profiles are chosen such that the mass and momentum flux of the jet-boundary layer combination is conserved. The viscous analyses are coupled with a relaxation solution of the external inviscid flow. The inviscid solution used here resembles that of Ives and Melnick<sup>6</sup> and is briefly reviewed in order to introduce, in a sequential manner, the description of the coupling.

A schematic representation of the inviscid airfoil/jet flap combination with related nomenclature is shown in Figure (2). Solutions for the flow field in the inviscid limit are sought by numerical integration of the full isentropic, compressible flow equations written in terms of the perturbation potential  $\phi$ , scaled by the freestream velocity and chord, and arranged in the canonical form

$$(1 - q^2/a^2) \phi_{ss} + \phi_{nn} = 0 \quad (7)$$

where  $s$  and  $n$  are orthogonal streamline coordinates,  $a$  is the local sound speed and  $q$  is the total velocity.

For the inviscid problem the boundary conditions along the airfoil and along the jet are, respectively, (it will be seen below that the coupling procedure will manifest itself only in a change in boundary conditions)

$$[\phi_y / (1 + \phi_x)]_{\ell, u} = f'_{\ell, u}(x) \quad (8)$$

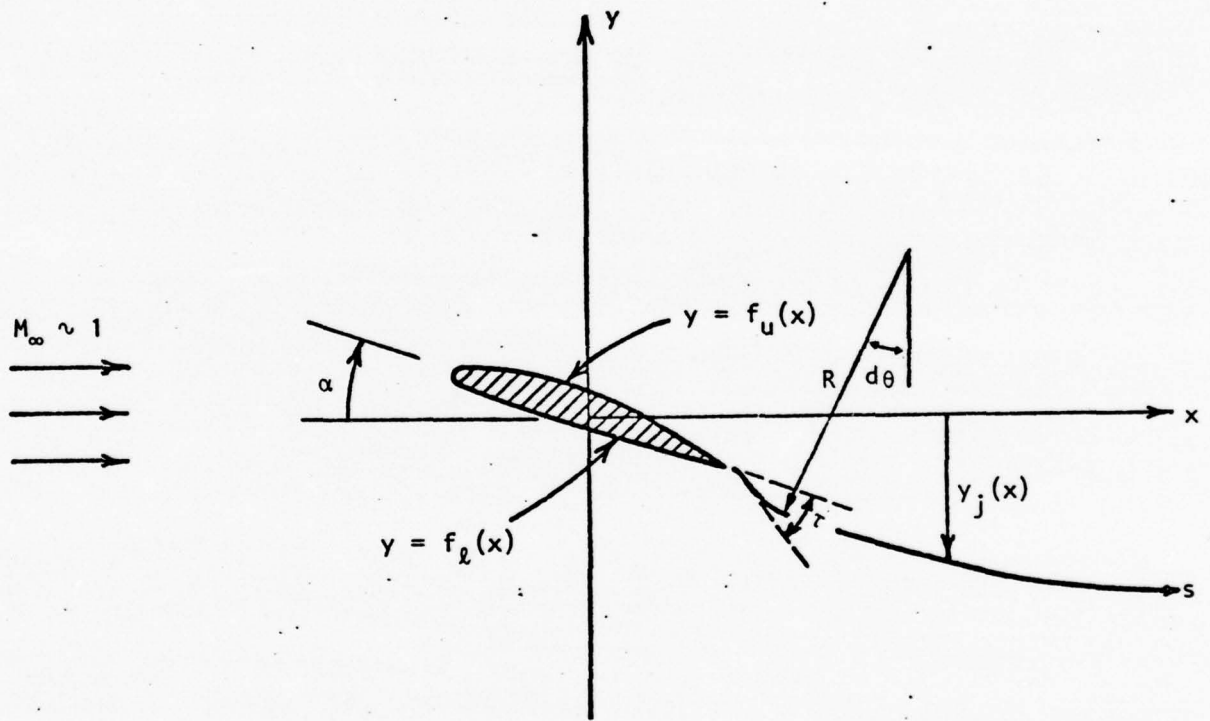


FIGURE 2. SCHEMATIC REPRESENTATION OF THE INVISCID JET-FLAPPED AIRFOIL

and

$$[\phi_y / (1 + \phi_x)]_j = y_j'(x). \quad (9)$$

Also, the pressure difference across the jet is required to satisfy the centrifugal force balance

$$\Delta c_p = -c_j/R \quad (10)$$

where  $c_j$  is the jet momentum per unit width (divided by the free stream dynamic pressure  $1/2 \rho_\infty U_\infty^2$  times the airfoil chord  $c$ ) and  $R$  is the dimensionless (scaled to  $c$ ) radius of curvature of the jet. Finally, boundary conditions are imposed at infinity. For  $M_\infty < 1$ , when the problem is inherently elliptic, the standard linearized vortex solution is imposed on the far field potential, viz.

$$\phi_\infty = -\frac{(\Gamma_a + \Gamma_j)}{2\pi} \tan^{-1} \frac{y_\infty \sqrt{1 - M_\infty^2}}{x_\infty} \quad (11)$$

where  $\Gamma_a$  is the circulation about the airfoil and  $\Gamma_j$  is the circulation about the jet sheet.

To numerically solve the system (7) - (11), a transformation from physical space into a unit square is performed. The mapping functions are

$$\begin{aligned} \xi &= \tanh(\alpha_1 x) \\ \eta &= \tanh\{\alpha_2 [y - g(x)]\} \end{aligned} \quad (12)$$

where

$$g(x) = \begin{cases} y_{L.E.} & \text{for } x < x_{L.E.} \\ f_u(x) & \text{for } x_{L.E.} < x < x_{T.E.}, y > f_u(x) \\ f_l(x) & \text{for } x_{L.E.} < x < x_{T.E.}, y < f_l(x) \\ y_j(x) & \text{for } x > x_{T.E.} \end{cases}$$

A schematic representation of the computational plane is shown in Figure (3).

The solution of Equation (7) is performed in  $\xi, \eta$  using the rotated difference technique of Jameson<sup>17</sup>. Tridiagonal equations of the form

$$a\phi_{i,j-1} + b\phi_{i,j} + c\phi_{i,j+1} = d \quad (13)$$

are derived, where  $a, b, c$  and  $d$  are functions of the coordinates and the previous iteration values.

The jet boundary condition, Equation (10), is incorporated into the difference scheme following the approach of Ives and Melnick. Across the jet

$$\phi_T = \phi_B + \Gamma(s) \quad (14)$$

where the subscripts T and B denote the top and bottom of the jet sheet, respectively, and  $\Gamma$  denotes the circulation at a given streamwise station along the jet. Since

$$\frac{d\Gamma}{ds} = q_T - q_B$$

and

$$ds = R d\theta$$

Equation (14) can be combined with Equation (10) and integrated to yield

$$\Gamma_j = \Gamma_{TE} + c_j \int_{\theta_{TE}}^{\theta} \left[ \frac{q_T - q_B}{c_{p_B} - c_{p_T}} \right] d\theta \quad (15)$$

Accordingly, the finite difference approximation to Equation (7) just below and just above the jet becomes

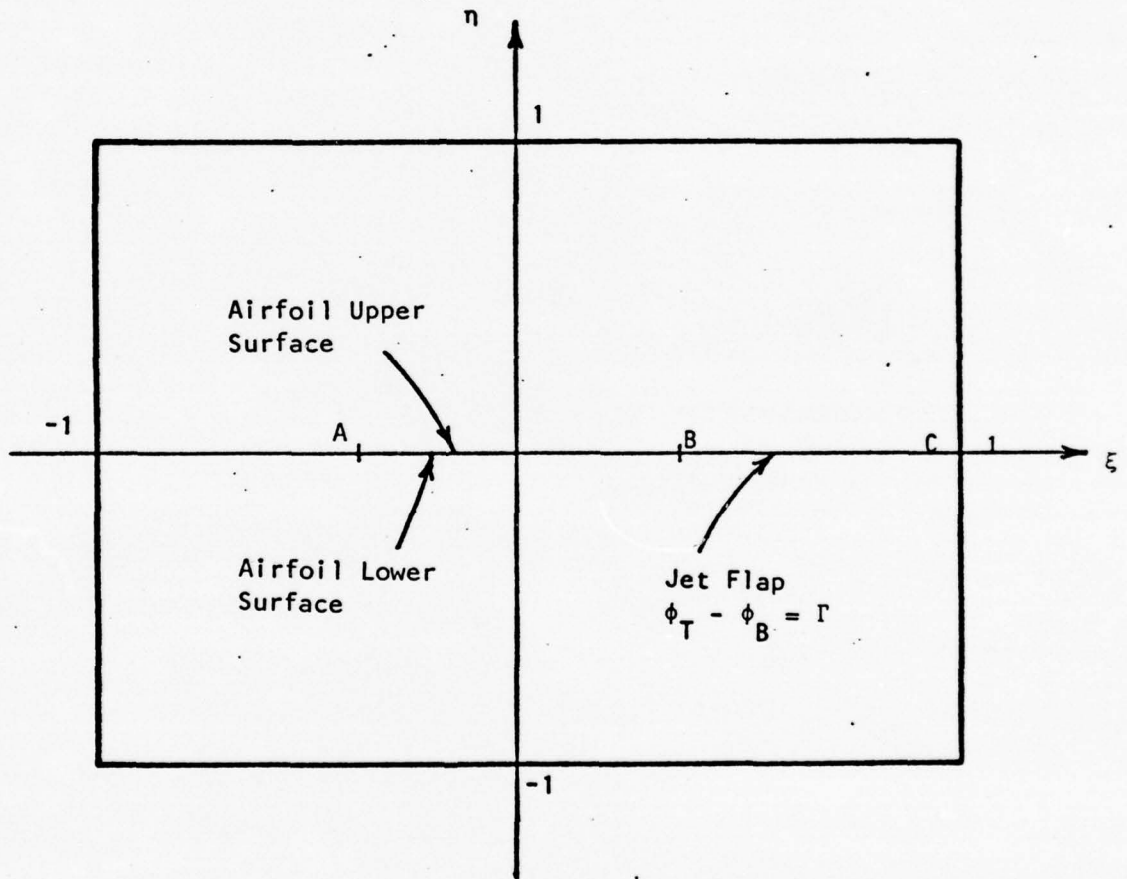


FIGURE 3. SCHEMATIC OF THE  $\epsilon, \eta$  COMPUTATIONAL PLANE

$$a_B \phi_{i,j-1} + b_B \phi_{i,j} + c_B \phi_{i,j+1} = d_B \quad (16)$$

$$a_T \phi_{i,j-1_T} + b_T \phi_{i,j_T} + c_T \phi_{i,j+1} = d_T$$

where  $\phi_{i,j+1_B}$  and  $\phi_{i,j-1_T}$  are fictitious points outside the flow field, and where  $\phi_{i,j_B}$  and  $\phi_{i,j_T}$  are the values of the potential just below and just above the jet, respectively.

The requirement that the velocity normal to the jet sheet is continuous across the sheet yields an additional relation which, once combined with Equations (15) and (16), eliminates the fictitious potentials  $\phi_{i,j+1_B}$  and  $\phi_{i,j-1_T}$ . Thus, the difference formulation

$$a_T \left(1 + \frac{a_B}{c_B}\right) \phi_{i,j-1} + \left(b_T + \frac{b_B a_T}{c_B}\right) \phi_{i,j} + (a_T + c_T) \phi_{i,j+1} = \quad (17)$$

$$\frac{a_T d_B}{c_B} + d_T - b_T \Gamma_j + a_T \frac{\alpha_1}{\alpha_2} \Delta \eta (1 - \xi^2) \sin 2\theta (\phi_T - \phi_B)_\xi$$

valid along the jet flap is achieved. The jet shape is obtained by tracing the streamline coming off the airfoil trailing edge and is updated during each interaction.

The coupling of the viscous results to the inviscid analysis is accomplished by a modification of the boundary conditions along the airfoil (Equation 8) and the jet (Equations 10 and 17). For the flow over the wing, a strong interaction coupling is utilized. The integral of the continuity equation in the viscous region yields

$$\frac{v_e}{u_e} = \frac{d\delta^*}{dx} - (\delta - \delta^*) \frac{d \ln(\rho_e u_e)}{dx} \quad (18)$$

In addition, as shown in Reference (11), one can express the displacement distribution in the form

$$\frac{d\delta^*}{dx} = \beta_1 + \beta_0 \frac{d \ln(\rho_e u_e)}{dx} \quad (19)$$

(where  $\beta_0$  and  $\beta_1$  are functions of the boundary layer quantities  $c_f$ ,  $\pi$ ,  $\delta^*$  for attached flow and  $P$  and  $\delta^*$  for separated flows, see References 11 and 12). Combining Equations (18) and (19) yields

$$\frac{v_e}{u_e} = \beta_1 + \beta_2 \frac{d \ln(\rho_e u_e)}{dx}$$

where  $\beta_2 = \beta_0 - (\delta - \delta^*)$ . Thus, the inviscid flow boundary condition

$$\phi_y = f'(x)$$

on the surface of the airfoil with profile  $y = f(x)$  is replaced by

$$\phi_y = f'(x) + \beta_1 + \beta_3 \phi_{xx} \quad (20)$$

where  $\beta_3 = \beta_2 (1 + M_\infty^2)$ , along the line  $y = f(x) + \delta^*(x)$ , or by the condition

$$\phi_y^v - \beta_3^{v-1} \phi_{xx}^v = f' + \beta_1^{v-1}$$

where the superscript  $v$  denotes the current iteration step. The coupling of inviscid and viscous flows is provided by the coefficients  $\beta_1$  and  $\beta_2$  and by the distribution  $\delta^*(x)$  (through the positioning of the boundary condition) which are functions of the boundary layer properties (but not of their gradients). This method of coupling is similar in philosophy to that of Tai<sup>18</sup> in that the viscous effect on displacement (through the variable  $v_e$ ) is directly incorporated into the solution for the inviscid field. It is also noted that in the "full" solution of the Navier-Stokes equations, Dewart<sup>19</sup> utilizes the

flow velocity  $v_e$  at the edge of the "viscous" layer directly to determine the outer flow properties.

With regard to the viscous-inviscid interaction along the jet, the two effects of momentum and mass entrainment must be recognized and incorporated directly into the coupling procedure. The first modifies the definition of  $c_j$ . The second is the sink effect and implies a discontinuity of normal velocity across the viscous jet. To determine the effect of entrainment on the jet momentum consider the equation for pressure across the jet

$$\frac{\partial p}{\partial n} = - \rho u^2 / R$$

and integrate it (in inner viscous variables) to yield

$$\Delta p \int_{-\infty}^{\infty} = - \int_{-\infty}^{\infty} \frac{\rho u^2}{R} dn .$$

But, from the outer (inviscid) solution

$$p_{\infty} = p_1 + \left(\frac{\partial p}{\partial n}\right)_1 n_{\infty} + \dots$$

$$p_{-\infty} = p_2 + \left(\frac{\partial p}{\partial n}\right)_2 n_{-\infty} + \dots$$

where

$$\left(\frac{\partial p}{\partial n}\right)_1 = - \rho_1 u_1^2 / R$$

$$\left(\frac{\partial p}{\partial n}\right)_2 = - \rho_2 u_2^2 / R .$$

Thus, the effect of mixing on the pressure difference across the jet can be expressed by the relationship

$$\Delta c_p = -\frac{1}{R} \left\{ \int_{\delta_2}^0 \frac{(\rho u^2 - \rho_2 u_2^2)}{\rho_\infty U_\infty^2 / 2} dn + \int_0^{\delta_1} \frac{(\rho u^2 - \rho_1 u_1^2)}{\rho_\infty U_\infty^2 / 2} dn \right\}$$

which replaces Equation (10). Note that for  $\rho u^2 \gg \rho_1 u_1^2, \rho_2 u_2^2$ , this expression reduces in the inviscid limit to  $\Delta c_p = -c_j/R$ . Then, if an "effective" momentum coefficient  $\bar{c}_j$  is defined, viz.

$$\bar{c}_j(s) = \int_{\delta_2}^0 \frac{(\rho u^2 - \rho_2 u_2^2)}{\rho_\infty U_\infty^2 / 2} dn + \int_0^{\delta_1} \frac{(\rho u^2 - \rho_1 u_1^2)}{\rho_\infty U_\infty^2 / 2} dn,$$

Equation (15) can be replaced by

$$\Gamma_j^v = \Gamma_{T.E.}^v + \int_{\theta_{T.E.}}^{\theta} \frac{\bar{c}_j^{v-1}(s) (q_T^v - q_B^v)}{(c_{p_B}^v - c_{p_T}^v)} d\theta \quad (21)$$

to account for momentum entrainment.

The sink effect is accounted for by imposing along the jet baseline the normal velocity discontinuity

$$(\Delta v)^v = v_{\delta_2}^{v-1} - v_{\delta_1}^{v-1} \quad (22)$$

where  $v_{\delta_2}$  and  $v_{\delta_1}$  are obtained by integrating the continuity equation from the base streamline. Thus

$$\left(\frac{v}{u}\right)_{\delta_2} = \frac{d \delta_2^*}{ds} - (\delta_2 - \delta_2^*) \frac{d \ln(\rho_2 u_2)}{ds} \quad (23)$$

$$\left(\frac{v}{u}\right)_{\delta_1} = \frac{d \delta_1^*}{ds} - (\delta_1 - \delta_1^*) \frac{d \ln(\rho_1 u_1)}{ds}$$

where

$$\delta_1^* = \int_0^{\delta_1} \left(1 - \frac{\rho u}{\rho_1 u_1}\right) dn$$

$$\delta_2^* = \int_0^{\delta_2} \left(1 - \frac{\rho u}{\rho_2 u_2}\right) dn$$

The finite difference form of the transonic equation, Equation (7), along the jet baseline then becomes

$$a_T \left(1 + \frac{a_B}{c_B}\right) \phi_{i,j-1} + \left(b_T + \frac{d_B a_T}{c_B}\right) \phi_{i,j} + (a_T + c_T) \phi_{i,j+1} =$$

$$\frac{a_T d_B}{c_B} + d_T - b_T \Gamma_j + a_T \frac{\alpha_1}{\alpha_2} \Delta \eta (1 - \xi^2) \sin 2\theta (\phi_T - \phi_B)_{\xi}$$

$$- 2a_T \cos \theta \frac{\Delta \eta}{\alpha_2} \overline{\Delta v} \quad (24)$$

where  $\Gamma_j$  and  $\overline{\Delta v}$  are given by Equations (21) and (22), respectively, in terms of values established at a preceding viscous iteration step.

The replacement of Equations (8) and (17) with Equations (20) and (24) constitutes the entire change in the inviscid program to account for strong

viscous interaction. The effects of viscosity are contained in the coefficient  $\beta_1$  and  $\beta_3$  of Equation (20) and the coefficients  $\overline{c_j}$  and  $\overline{\Delta v}$  of Equations (21) and (22). The values of these coefficients are obtained from the viscous analysis along the airfoil and along the jet, developed in Reference (12) and in the present report.

TR 237  
SECTION IV  
RESULTS AND CONCLUSIONS

In Reference (11), preliminary results were reported to ascertain the importance of viscous effects in the analysis of jet-flapped airfoils in the transonic regime. For the airfoil without a jet flap the viscous interaction model along the airfoil was validated by the results shown in Figure (4) relative to a 6% circular-arc airfoil at  $M_\infty = 0.908$ . The numerical result agree quite favorably with the experiment of Reference (20). The influence of jet mixing on the pressure distribution over the wing can be of equal importance, as manifested by the result of Figure (5) which presents the pressure distribution over an airfoil at zero angle of attack without and with a straight jet flap. Additional results have now been obtained by use of the analysis developed in the previous sections.

The influence of mass and momentum entrained by the jet on the pressure distribution over an airfoil was studied by examining the flow about a 12% thick circular-arc airfoil (which is similar to a NACA 0012 except at the nose) at zero angle of attack with a jet flap having an initial deflection angle of  $30^\circ$ , a jet-momentum coefficient  $c_j = 0.1$  and a mass flow rate  $\rho_j u_j \delta_j / \rho_\infty U_\infty c = 0.04$ , at a free stream Mach number of 0.7. Figure (6) presents the pressure distribution over the airfoil for the case of an inviscid, infinitely thin jet flap and of a viscous jet flap. For the viscous jet, the pressure distribution along the upper and lower jet boundaries are given in Figure (7). Also shown in the figure are the corresponding components of the normal velocity as computed by Equation (23) of the viscous analysis. Note that for this case (a moderate  $c_j$  and a moderate deflection angle), the sink effect near the trailing edge changes the initial deflection angle by about 6% (since  $\tan 30^\circ = 0.577$  and  $(\frac{v}{U})_{\max} \sim 0.034$ ). Note also that this effects damps quickly to extremely small values in a distance of about 20% of the chord.

The results of Figure (6) indicate that the pressure distribution on the top-aft section of the airfoil is slightly altered, while that on the bottom-aft section is essentially unaffected. The lower pressure on the aft-top surface results in a decrease in thrust, as compared with the inviscid case, while the

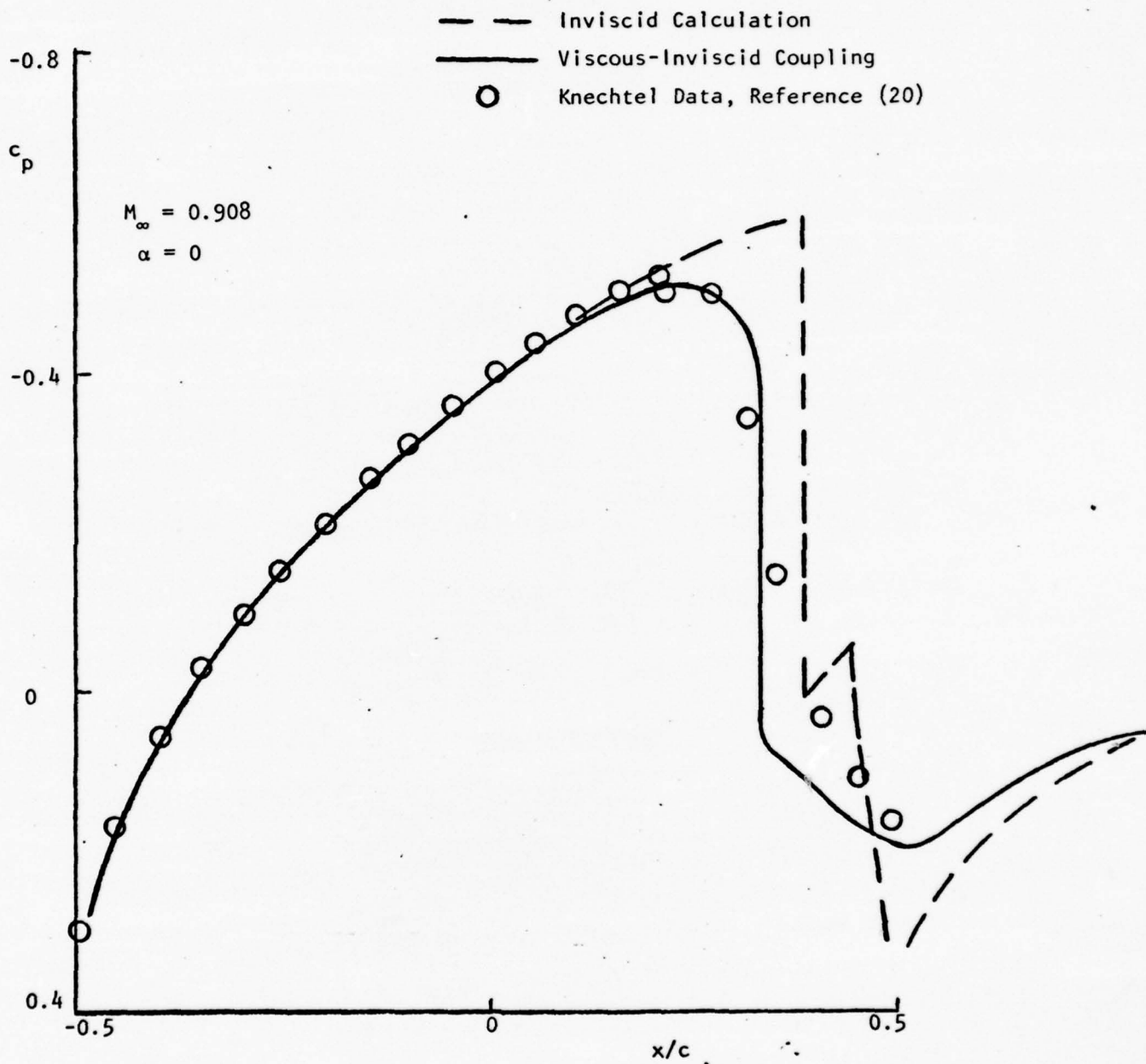


FIGURE 4. EFFECTS OF VISCOUS-INVISCID INTERACTION ON 6% CIRCULAR-ARC AIRFOIL

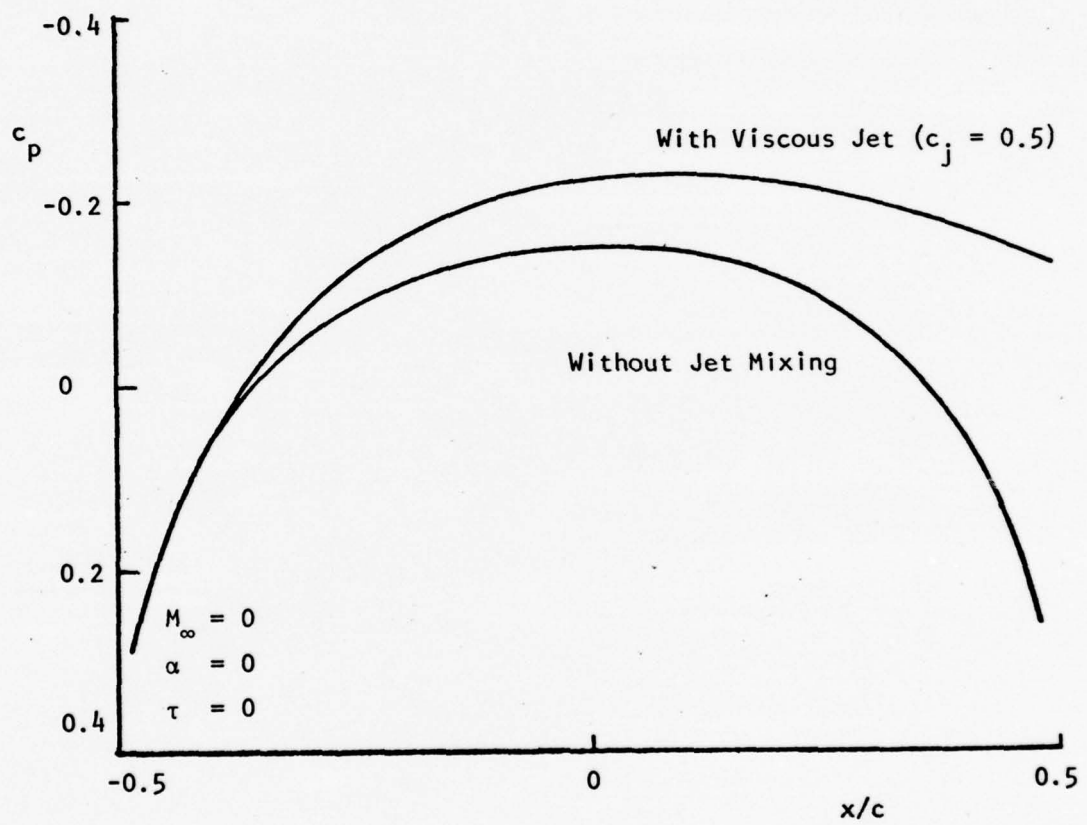


FIGURE 5. EFFECT OF JET MIXING ON PRESSURE DISTRIBUTION OVER A 6% CIRCULAR-ARC AIRFOIL

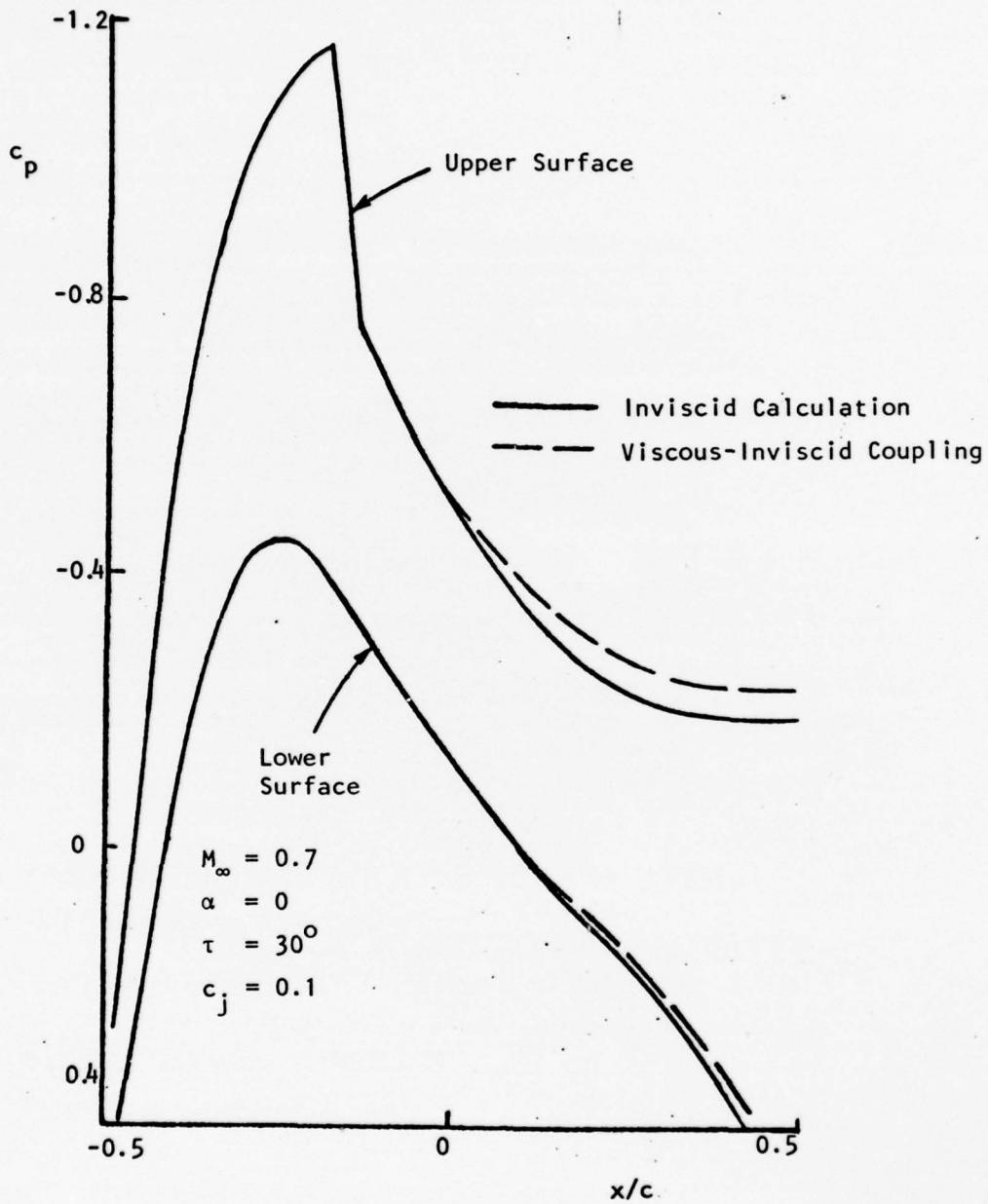


FIGURE 6. EFFECT OF JET VISCOSITY ON PRESSURE DISTRIBUTION OVER A 12% CIRCULAR-ARC AIRFOIL

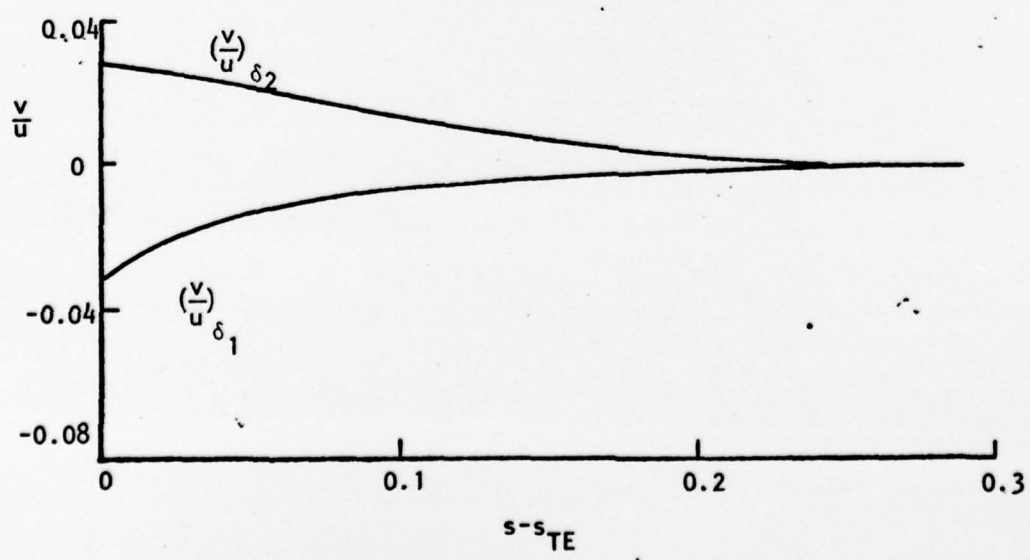
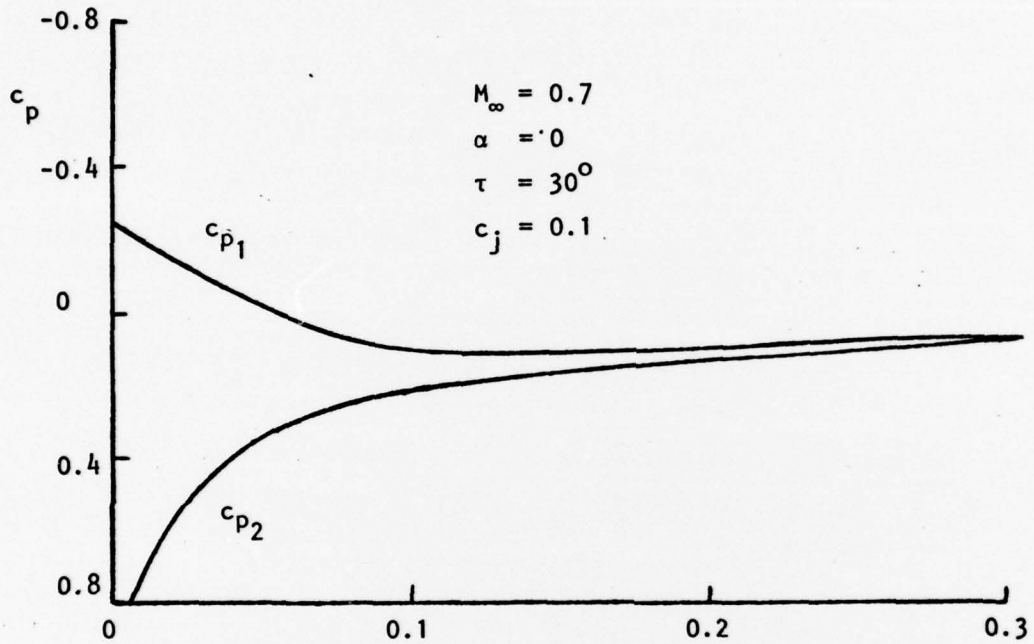


FIGURE 7. PRESSURES AND NORMAL VELOCITIES ALONG BOUNDARIES OF JET MIXING REGION

lift is somewhat enhanced. The calculation also indicates that, for this particular case, the effect of momentum entrainment by the jet is small and, to first order, the jet momentum as a function of position (e.g. the  $\overline{c_j}(s)$  coefficient in Equation (21)) is approximately equal to the initial jet momentum  $c_j$ . This fact may not be true for much smaller values of  $c_j$ , i.e. for  $c_j \ll 0.1$ . The major effect of entrainment is due to the sink effect (the parameter  $\Delta v$  of Equation (22)) whose magnitude can be ascertained from Figure (7). The effect of jet entrainment is more pronounced on the airfoil upper surface than on the lower surface, since the flow around the lower surface must experience a large pressure increase near the trailing edge because of the initial jet deflection, while the upper surface exhibits a relief on adverse gradient due to the jet. The top surface is also more susceptible to the ejector effect of the jet flap. In addition, the sink effect is proportional to the magnitude of  $c_j$  as indicated by numerical experiments carried with the present analysis. Thus, for a given initial jet deflection angle the effect of viscosity, through mass entrainment, increases with increasing jet momentum.

The other parameter whose variation can significantly alter the effect of entrainment is the initial jet deflection angle  $\tau$ . As  $\tau$  increases, the inviscid effects of rear stagnation on the bottom surface and of pressure relief on the top surface become more and more pronounced. At the same time, the effect of the jet on separation and bubble development is enhanced. Thus, as pointed out in Reference (10), the identity of the jet can be obliterated by viscous mixing. It therefore seems that the effect of viscosity is important for small (see Figure 5) and large (see Reference 10) jet deflection angles. Thus, one can expect the effects of entrainment will be most significant for large  $c_j$  and for both small and large  $\tau$ . Therefore, a program which computes the viscous-inviscid interaction is necessary to properly ascertain the lift and thrust increments (or decrements) under a particular set of conditions. The coupling procedure described in the previous section for the airfoil and the jet, when utilized in concert, can adequately describe the effects of viscosity and can be readily incorporated into existing codes for an assessment of jet flap performance for flows without large separation. In addition, as pointed out in Reference (10), a proper assessment of viscous effects for the treatment

TR 237

of jet-flapped wings of finite span would entail the development of a three-dimensional analysis, perhaps utilizing some of the concepts developed herein.

## REFERENCES

1. Yoshihara, H., Zonars, D. and Carter, W., "High Reynolds Number Transonic Performance of Advanced Planar Airfoils with Jet-Flaps," AFFDL TR 71-61, June 1971.
2. Peake, D., Yoshihara, H., Zonars, D. and Carter, W., "The Transonic Performance of 2D Flapped Aerofoils at High Reynolds Numbers," AGARD CP No. 83, August 1971.
3. Yoshihara, H., Magnus, R. and Zonars, D., "Transonic Drag due to Lift of Planar Jet-Flapped Airfoils," AGARD CP No. 124, 1973.
4. Yoshihara, H., Benepe, D. and Whidden, P., "Transonic Performance of Jet-Flaps on Advanced Fighter Configuration," AFFDL TR-73-97, 1973.
5. Peake, D. J., Bowker, A. J., Mokry, M., Yoshihara, H. and Magnus, R., "Transonic Lift Augmentation of Two-Dimensional Supercritical Aerofoils by Means of Aft Camber, Slot Blowing and Jet-Flaps, in High Reynolds Number Flow," ICAS Paper No. 74-11, Haifa, Israel, August 1974.
6. Ives, D. D. and Melnick, R. E., "Numerical Calculation of the Compressible Flow over an Airfoil with a Jet-Flap," AIAA Paper No. 74-542, June 1974.
7. Malmuth, N. D. and Murphy, W. D., "A Relaxation Solution for Transonic Flow over Jet-Flapped Airfoils," AIAA Journal, Vol. 14, No. 9 September 1976.
8. Malmuth, N. D. and Murphy, W. D., "Relaxation Solution for Transonic Flow over Three-Dimensional Jet-Flapped Wings," AIAA Journal, Vol. 15, No. 1, January 1977.
9. Stratford, B. S., "Mixing and the Jet-Flap," The Aeronautical Quarterly, Vol. VII, 1956.
10. Yoshihara, H. and Zonars, D., "The Transonic Jet Flap - A Review of Recent Results," SAE Transactions, Vol. 84, Section 4, Paper No. 75189, 1975.
11. Elzweig, S., Baronti, P. and Miller, G., "An Analysis of Transonic Jet-Flapped Airfoils with the Inclusion of Viscous Effects," ATL TR 230, May 1976.
12. Miller, G. and Baronti, P., "Solution of Transonic Separating Turbulent Boundary Layers," ATL TR 214, May 1975.
13. Baronti, P. and Miller, G., "Integral Solution of the Turbulent Kinetic Energy Equation," AIAA Journal, Vol. 12, No. 1, January 1974.
14. Ting, L., "On the Mixing of Two Parallel Streams," Journal of Mathematical Physics, Vol. 38, No. 3, October 1959.

REFERENCES (Continued)

15. Bradshaw, P., Ferris, D. H. and Atwell, N. P., "Calculation of Boundary Layer Development Using the Turbulent Energy Equation," *Journal of Fluid Mechanics*, Vol. 28, Part 3, 1967.
16. Bradshaw, P. and Ferris, D. H., "Calculation of Boundary-Layer Development Using the Turbulent Energy Equation: Compressible Flow on Adiabatic Walls," *Journal of Fluid Mechanics*, Vol. 46, Part 1, 1971.
17. Jameson, A., "Transonic Potential Flow Calculations Using Conservation Form," *Procs. AIAA 2nd Computational Fluid Dynamics Conference*, Hartford, CT, June 1975.
18. Tai, T. C., "Transonic Turbulent Viscous-Inviscid Interaction over Airfoils," *AIAA Paper No. 75-78*, January 1975.
19. Deiwert, G. S., "Numerical Simulation of High Reynolds Number Transonic Flows," *AIAA Journal*, Vol. 13, No. 10, October 1975.
20. Knechtel, E. D., "Experimental Investigation at Transonic Speeds of Pressure Distributions over Wedge and Circular-Arc Airfoil Sections and Evaluation of Perforated-Wall Interference," *NASA TN-D-15*, August 1959.

COMPRESSIBILITY TRANSFORMATIONS AND CROCCO  
RELATION FOR VISCOUS JET ANALYSIS

A restricted Dorodnitsyn-Howarth transformation

$$\begin{aligned}\bar{s} &= s \\ \bar{n} &= \int_0^n \rho/\bar{\rho} \, dn \\ \bar{\psi} &= \psi\end{aligned}\tag{A,1}$$

with barred quantities denoting transformed values, is utilized here to account for compressibility effects along the jet.

The transformation implies that

$$\bar{u} = u$$

and

$$\bar{v} = \frac{v\bar{\rho}}{\rho} + \bar{u} \frac{\partial \bar{n}}{\partial s}$$

Then, if it is further assumed that  $\tau = \bar{\tau}$ , the momentum equation along the jet becomes (to order  $\delta$ )

$$\bar{u} \frac{\partial \bar{u}}{\partial \bar{s}} + \bar{v} \frac{\partial \bar{u}}{\partial \bar{n}} = - \frac{1}{\rho} \frac{\partial p}{\partial \bar{s}} + \frac{1}{\rho} \frac{\partial \bar{\tau}}{\partial \bar{n}}\tag{A,2}$$

Since across the jet

$$\frac{\partial p}{\partial \bar{n}} = - \rho \frac{u^2}{R},$$

application of the transformation also implies

$$\frac{\partial p}{\partial \bar{n}} = - \frac{\rho u^2}{R} \quad (\text{A,3})$$

and thus

$$\frac{\partial p}{\partial \bar{n}} = \frac{\partial \bar{p}}{\partial \bar{n}}$$

It then also follows that

$$\frac{\partial p}{\partial \bar{s}} = \frac{\partial \bar{p}}{\partial \bar{s}} = \frac{\partial p}{\partial s}$$

The density term  $1/\rho$  in the momentum equation can be expressed directly in terms of velocity and pressure profiles and of edge conditions by invoking the local validity of the Crocco integral. One then has

$$\frac{1}{\rho} = \frac{1}{p} \left[ Au + B - \frac{\gamma-1}{2\gamma} u^2 \right] \quad (\text{A,4})$$

where

$$A = \frac{(p_1/\rho_1 - p_2/\rho_2)}{u_1 - u_2} + \frac{\gamma-1}{2\gamma} (u_1 + u_2)$$

$$B = \frac{(p_2/\rho_2 u_1 - p_1/\rho_1 u_2)}{u_1 - u_2} - \frac{\gamma-1}{2\gamma} u_1 u_2$$

INTEGRAL METHOD FOR CURVED JET

Integration of the transformed momentum equation, Equation (A,2), between 0 and  $\bar{\delta}_1/2$ , 0 and  $\bar{\delta}_2/2$  and between  $\bar{\delta}_1$  and  $\bar{\delta}_2$  yields (for convenience, all transformed quantities are now indicated by unbarred symbol whereas  $\tilde{\rho}$  indicates the compressible density)

$$\begin{aligned} \frac{d}{ds} \int_0^{\delta_i/2} u^2 dn = u_{\delta_i/2} \frac{d}{ds} \int_0^{\delta_i/2} udn = \\ - \int_0^{\delta_i/2} \frac{1}{\tilde{\rho}} \frac{\partial p}{\partial s} dn + (\tau/\rho)_{\delta_i/2} - (\tau/\rho)_0 \end{aligned} \quad (B,1)$$

where  $i = 1, 2$ , and

$$\begin{aligned} \frac{d}{ds} \int_{\delta_2}^{\delta_1} u^2 dn - u_1 \frac{d}{ds} \int_0^{\delta_1} udn + u_2 \frac{d}{ds} \int_0^{\delta_2} udn = \\ - \int_{\delta_2}^{\delta_1} \frac{1}{\tilde{\rho}} \frac{\partial p}{\partial s} dn \end{aligned} \quad (B,2)$$

The density  $\tilde{\rho}$  has been defined above by Equation (A,4), the velocity profiles are expressed by the polynomial

$$u = u_0 + a_1 n + a_2 n^2 \quad (B,3)$$

where  $u_0$  is the velocity along the "base" streamline and where the coefficients  $a_1$  and  $a_2$  are obtained by satisfying the boundary conditions  $u=u_1$  at  $n=\delta_1$  and  $u=u_2$  at  $n=\delta_2$  to yield

$$a_1 = [(u_1 - u_0) \delta_2^2 - (u_2 - u_0) \delta_1^2] / D$$

$$a_2 = [(u_2 - u_0) \delta_1 - (u_1 - u_0) \delta_2] / D$$

$$D = \delta_1 \delta_2^2 - \delta_2 \delta_1^2$$

The pressure distribution across the layer can be obtained by integrating the normal momentum equation (A,3) to yield a fifth-order polynomial for  $p$ . This was originally proposed in Reference (11). It was felt, however, that since  $\partial p / \partial n$  cannot change sign across the layer, it may be possible to lower the order of the polynomial. Extensive investigation has indicated that a linear solution is adequate. A pressure distribution of the form

$$p = \frac{1}{(\delta_1 - \delta_2)} [(p_2 \delta_1 - p_1 \delta_2) + (p_1 - p_2) n] \quad (B,4)$$

has been, henceforth, utilized here.

Thus, by inserting Equations (A,4), (B,3) and (B,4) into Equations (B,1) and (B,2) and performing the integrations and differentiations one obtains the system of equations

$$a_{11} \frac{du_0}{ds} + a_{12} \frac{d\delta_1}{ds} + a_{13} \frac{d\delta_2}{ds} = C_1$$

$$a_{21} \frac{du_0}{ds} + a_{22} \frac{d\delta_1}{ds} + a_{23} \frac{d\delta_2}{ds} = C_2 \quad (B,5)$$

$$a_{31} \frac{du_0}{ds} + a_{32} \frac{d\delta_1}{ds} + a_{33} \frac{d\delta_2}{ds} = C_3$$

which defines the flow variables  $u_0$ ,  $\delta_1$  and  $\delta_2$ .

To obtain the shear distribution and, thus, the values  $\tau_{\delta_1/2}$ ,  $\tau_{\delta_2/2}$  and  $\tau_0$  appearing in Equations (B,1) and (B,2) it is assumed that (unbarred quantities shall indicate transformed values).

$$\tau/\rho = b_0 + b_1 n + b_2 n^2 + b_3 n^3 \quad (\text{B},6)$$

The coefficient  $b_1$  is obtained by satisfying the  $s$ -momentum equation along the  $n = 0$  line; hence

$$b_1 = \left( \frac{\partial \tau}{\partial n} \right)_0 = u_0 \frac{du_0}{ds} + \frac{1}{\rho_0} \left( \frac{\partial p}{\partial s} \right)_0$$

The coefficients  $b_0$  and  $b_2$  are obtained by satisfying the boundary conditions

$$\tau = 0 \text{ at } y = \delta_1, \delta_2.$$

Hence,

$$b_0 = \frac{1}{D_2} \{ -(b_1 \delta_1 + b_3 \delta_1^3) \delta_2^2 + (b_1 \delta_2 + b_3 \delta_2^3) \delta_1^2 \}$$

$$b_2 = \frac{1}{D_2} \{ -(b_1 \delta_1 + b_3 \delta_2^3) + (b_1 \delta_1 + b_3 \delta_1^3) \}$$

where

$$D_2 = \delta_2^2 - \delta_1^2$$

The coefficient  $b_3$  is then obtained by integrating the TKE equation (Equation B,5) across the viscous jet layer, viz.,

$$\begin{aligned} \frac{1}{2a_i} \frac{d}{ds} \int_{\delta_2}^{\delta_1} \frac{\tau}{\rho} u dn - \int_{\delta_2}^{\delta_1} \frac{\tau}{\rho} \frac{\partial u}{\partial n} dn \\ + \int_{\delta_2}^{\delta_1} \frac{(\tau/\rho)^{3/2}}{L} dn = 0 \end{aligned} \quad (\text{B},7)$$

with the parameters  $a_i$  and  $L$  given in Reference (15). By inserting Equations (B,3) and (B,6) into Equation (B,7), one then obtains the ordinary differential equation for  $b_3$  of the form

$$B_1 \frac{db_3}{ds} = G_1$$

Thus, Equations (B,5) and (B,7) provide the sought closure of equations and unknowns for the solution of  $\delta_1(s)$ ,  $\delta_2(s)$ ,  $u_0(s)$  and  $b_3(s)$  in the transformed plane.

UNCLASSIFIED

SECURITY CLASSIFICATION OF THIS PAGE (When Data Entered)

18 19 REPORT DOCUMENTATION PAGE		READ INSTRUCTIONS BEFORE COMPLETING FORM
1. REPORT NUMBER AFOSR - TR - 77 - 0446	2. GOVT ACCESSION NO.	3. RECIPIENT'S CATALOG NUMBER 9
4. TITLE (and Subtitle) 6 THE EFFECTS OF VISCOUS INTERACTION ON THE TRANSONIC JET-FLAP.		5. TYPE OF REPORT & PERIOD COVERED FINAL rept. 1 Oct 75 - 30 Sep 76
7. AUTHOR(s) 10 P. BARONTI, S. ELZWEIG, G. MILLER	14	6. PERFORMING ORG. REPORT NUMBER GASL-TR-237
9. PERFORMING ORGANIZATION NAME AND ADDRESS GENERAL APPLIED SCIENCE LABORATORIES, INC. MERRICK AND STEWART AVENUES WESTBURY, NEW YORK 11590	15	8. CONTRACT OR GRANT NUMBER(s) F44620-76-C-0017 new
11. CONTROLLING OFFICE NAME AND ADDRESS AIR FORCE OFFICE OF SCIENTIFIC RESEARCH/NA BLDG 410 BOLLING AIR FORCE BASE, D C 20332 12 43p.		10. PROGRAM ELEMENT, PROJECT, TASK AREA & WORK UNIT NUMBERS 16 9781 01 61102F 17
14. MONITORING AGENCY NAME & ADDRESS (if different from Controlling Office)		12. REPORT DATE 11 March 1977
		13. NUMBER OF PAGES 40
		15. SECURITY CLASS. (of this report) UNCLASSIFIED
		15a. DECLASSIFICATION/DOWNGRADING SCHEDULE
16. DISTRIBUTION STATEMENT (of this Report)  Approved for public release; distribution unlimited.		
17. DISTRIBUTION STATEMENT (of the abstract entered in Block 20, if different from Report)		
18. SUPPLEMENTARY NOTES		
19. KEY WORDS (Continue on reverse side if necessary and identify by block number) JET FLAPS TRANSONIC FLOW VISCOUS-INVISCID INTERACTION		
20. ABSTRACT (Continue on reverse side if necessary and identify by block number) The inviscid and viscous effects associated with a jet-flapped airfoil in the transonic regime are investigated. The particular formulation developed employs integral methods for the description of the viscous portions of the flow (utilizing the turbulent kinetic energy equation) and a relaxation method for the inviscid portions. The viscous-inviscid coupling procedures along the wing and the jet acknowledge the importance and magnitude of the viscous effects on pressure distribution and directly incorporate the displacement effect on the wing and the effects of the jet mixing into the boundary conditions for the computation.		

SECURITY CLASSIFICATION OF THIS PAGE(When Data Entered)

of the entire flow. Some numerical results are presented to validate the solution techniques that have been selected and to assess the importance of mass and momentum entrainment into the jet on jet flap effectiveness.

<p>10-1-1960</p>	<p>RESEARCH REPORT</p>

SECURITY CLASSIFICATION OF THIS PAGE(When Data Entered)

of the entire flow. Some numerical results are presented to validate the solution techniques that have been selected and to assess the importance of mass and momentum entrainment into the jet on jet flap effectiveness.

<p>11-10-68 - 11-10-68</p>	<p>CONFIDENTIAL</p>
<p>CONFIDENTIAL</p>	<p>CONFIDENTIAL</p>